Krypton $3p$ excitations and subsequent resonant Auger decay

R. Sankari, A. Kivimäki, H. Aksela, and S. Aksela
Department of Physical Sciences, P.O. Box 3000, 90014 University of Oulu, Finland

K. C. Prince
Sincrotrone Trieste, I-34012 Trieste, Italy
and INFM-TASC, Area Science Park, I-34012 Trieste, Italy

M. Coreno and M. Alagia
INFM-TASC, Area Science Park, I-34012 Trieste, Italy

M. de Simone
Dipartimento di Fisica "E. Amaldi," Università di Roma III, I-00146 Rome, Italy
and Unità INFM-TASC, Area Science Park, I-34012 Trieste, Italy
(Received 18 December 2002; published 21 March 2003)

Krypton $3p$ excitations and their subsequent resonant Auger decay have been studied. The absolute photoabsorption cross section was determined in the region of the $3p$ resonances, and some structures were detected in the absorption spectrum. Hartree-Fock calculations including correlation between $3p^{-1}nl$ and $3d^{-2}n'l'nl$ configurations were used to interpret the structures of the $3p$ resonant excitation series and of the corresponding decay spectra. Furthermore, the decay spectra confirmed the assignment of the main structures in the absorption spectrum.

DOI: 10.1103/PhysRevA.67.032710 PACS number(s): 32.80.Hd, 32.80.Fb

I. INTRODUCTION

During the 1970s, the experimental accuracy of electron spectroscopic studies increased strongly. Very soon experiments revealed anomalous behavior of certain photoelectron lines of xenon and krypton, which was later explained by the breakdown of the independent particle model. For example, the Kr $3p$ photoelectron spectrum measured by Svensson *et al.* [1] showed that the $3p$ photoelectron lines consist of many components that arise due to strong mixing of the $3p^{-1}$ and $3d^{-2}\epsilon f$ states [2], similarly to more widely studied Xe $4p$ photoionization (see, e.g., Refs. [3–5]). However, the experimental Kr absorption spectrum [6,7] measured below the $3p$ threshold has so far been theoretically explained successfully within the one-electron picture by Ohno [8] and Hayaishi *et al.* [6], although they give different assignments for the structures of the absorption spectrum. Due to the much higher photon energy resolution than in the experimental study of Steinberger *et al.* [7], the present measurements reveal some features in the absorption spectrum at the Kr $3p$ ionization threshold. A recent high-resolution total ion yield spectrum (TIY) reported by Matsui *et al.* [9] also gave a hint of such structures but they were nevertheless omitted in the analysis of the spectrum.

Experimental investigations of Jauhiainen *et al.* [10] and Brünken *et al.* [11] show that the Kr $3p$ core ionized states decay mainly by the Coster-Kronig or super-Coster-Kronig transitions resulting in large linewidths in the decay spectra. However, in the case of core-excited states the Auger resonant Raman effect can be utilized to sharpen the structures of the decay spectra beyond the limit defined by the natural lifetime widths of the excited states.

In the present work, absorption and resonant Auger spectra of krypton were recorded at photon energies corresponding to the $3p$ excitations. The resonant Auger decay channels to the $3d^{-1}4s^{-1}nl$ and $3d^{-1}4p^{-1}nl(n\geqslant 4)$ states of Kr were investigated in detail. Hartree-Fock (HF) calculations including configuration interaction were performed to interpret the structures of the absorption spectrum and resonant Auger decay spectra.

II. EXPERIMENT

The measurements were carried out at the gas phase photoemission beam line of the ELETTRA storage ring in Trieste, Italy. An undulator source provides high-intensity synchrotron radiation in the photon energy range 20–900 eV. The highly polarized light [12] is dispersed by a variable-angle spherical grating monochromator that is equipped with four interchangeable gratings, fixed entrance and exit slits, and prefocusing and postfocusing optics. The monochromatic synchrotron radiation can also be deflected to the branch line by a gold coated plane mirror. The usable photon energy range at the branch line is 14–240 eV. A more detailed description of the beam line can be found elsewhere [13].

The emitted electrons were analyzed by a VG220i hemispherical electron energy analyzer (mean radius of 150 mm) equipped with six channel electron multipliers. The electron energy analyzer was mounted at the branch line. For the resonant Auger measurements, the photon energy was set to correspond to different $3p$ excitations with the aid of the absorption measurements. The photoabsorption cross section depicted in Fig. 1 was measured with a Samson-type double

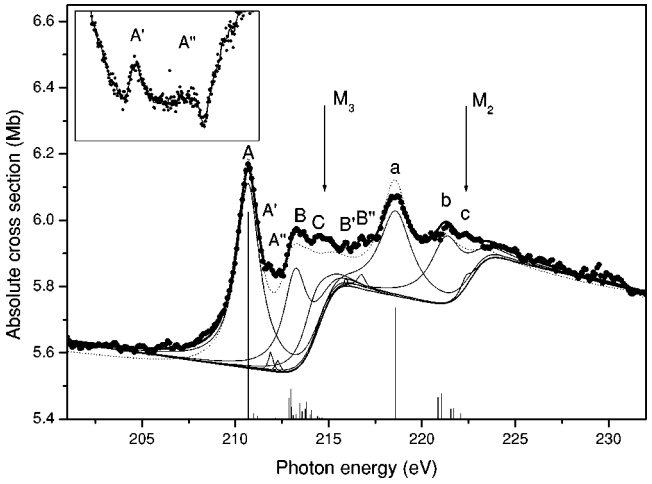

FIG. 1. $M_{2,3}$ preedge Rydberg excitations in Kr. Dots show the experimental data; the thick and thin solid lines give the least-squares fit for the whole spectrum and individual transitions, respectively. The dotted line represents a theoretical spectrum based on CI-I calculations, whereas columns represent the results of the CI-II calculations (see text for details). The arrows show the $M_{2,3}$ ionization limits [6]. The inset represents structures A' and A'' in detail.

cell [14,15] at the main line with entrance and exit slits set at 30 and 50 μm, respectively, corresponding to photon bandwidth of about 40 meV. The large background is due to the high continuum cross section for photoionization from the $3d$ orbitals. This illustrates one of the difficulties of absorption spectroscopy at this edge: the relatively weak features are superimposed on a large background. Both the resonant Auger and photoelectron spectra were measured with a photon bandwidth of about 50 meV. The pass energy of the electron energy analyzer was set at 3 eV, which resulted in an electron energy resolution of about 50 meV. The binding-energy scale was calibrated according to the Kr $3d$ photoelectron lines, whose binding energies $[E_B(3d_{3/2}) = 95.038$ eV and $E_B(3d_{5/2}) = 93.788$ eV] are known within an accuracy of ± 0.025 eV [16]. The photoelectron spectrum of krypton was also measured at a photon energy of about 15 eV below the $3p$ resonant excitations, where the intensity in the binding-energy region of interest is given mainly by direct $3d$ photoionization and associated shake-up satellites. All the electron spectra were corrected for the spectrometer transmission by using the ratios between the intensities of Kr $3d$ photoelectron and $M_{4,5}N_{2,3}N_{2,3}$ normal Auger-electron spectra [17].

III. RESULTS AND DISCUSSION

A. Absorption

The absorption spectrum in the region of the Kr $3p$ excitations is depicted in Fig. 1. The excitation energies and the widths of the most prominent features of the spectrum were extracted from the measurement. The experimental values are presented in Table I. In general, the agreement with earlier results of Steinberger *et al.* [7] is very good. However, in addition to the structures reported previously, we detected narrow peaks (A' and A'' in Fig. 1) between the strong components A and B. They seem to be present also in the recent high-resolution TIY spectrum of Matsui *et al.* [9], but the spectrum was not analyzed in detail. Some additional structures were also detected at higher photon energies (B' and B'' in Fig. 1). The absorption spectrum was recorded several times to verify these faint features.

HF calculations based on Cowan's code [18] were performed to assign the structures of the absorption spectrum. The first calculations included configuration interaction (CI) between the $3p^{-1}ns(n=5-7)$ and $3p^{-1}md(m=4-6)$ states (referred as CI-I calculations) whereas the larger configuration set included in addition the $3d^{-2}np(ns/md)$ configurations (referred as CI-II calculations). According to both calculations the most prominent broad peaks in the absorption spectrum were assigned to $3p \rightarrow ns$ and md excitations. The calculated excitation strengths to the $3p^{-1}md$ states were found to be weaker than the $3p \rightarrow ns$ excitations, as pointed out already in earlier studies [7,8]. However, both of the present calculations suggest that the $3p \rightarrow md$ excitations cannot be neglected as, for example, the theoretical $3p$

TABLE I. Experimental and theoretical (CI-II) energies and lifetime widths of Kr $3p^{-1}nl$ excited states. Labels refer to Fig. 1; all units are in eV. Theoretical energies are shifted down by 3.29 eV to aid comparison.

Label	Assignment	E_{exp}	E_{theory}	Γ_{exp}	Γ_{theory}
A	$3p_{3/2}^{-1}5s$	210.69(10)	210.69	1.4(1)	1.4
A'	$3d^{-2}7p4d$	211.67(5)	212.99	0.17(5)	0.18
A''	$3d^{-2}5p6s$	212.48(5)	213.46	0.17(5)	0.18
B	$3p_{3/2}^{-1}4d$	213.22(10)	212.88	1.4(1)	1.8
	$3p_{3/2}^{-1}6s$		213.01		1.4
C	$3p_{3/2}^{-1}5d$	214.26(10)	213.74	1.4(1)	1.8
	$3p_{3/2}^{-1}7s$		213.81		1.4
a	$3p_{1/2}^{-1}5s$	218.59(10)	218.56	1.9(1)	1.8
b	$3p_{1/2}^{-1}4d$	221.27(10)	220.85	1.9(1)	1.8
	$3p_{1/2}^{-1}6s$		221.04		1.8
c	$3p_{1/2}^{-1}5d$	222.36(10)	221.69	1.9(1)	1.8
	$3p_{1/2}^{-1}7s$		221.80		1.8

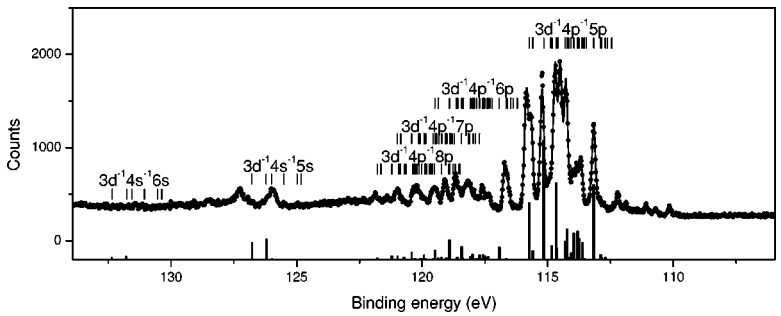

FIG. 2. Kr 3d photoelectron shake-up satellite spectrum measured at 195 eV photon energy. The theoretical shake-up spectrum based on sudden-approximation calculations is presented as columns. The theoretical spectrum has been shifted up by 0.84 eV to make the theoretical and experimental spectra coincide at a binding energy of 113.17 eV. Electron configurations are given above respective line groups.

$\rightarrow 4d$ excitation strength is almost equal to the $3p\rightarrow 6s$ excitation strength. In fact, only the existence of underlying $3p_{3/2}^{-1}4d$ and $5d$ excitations explains the high absorption in the region of the peak B in Fig. 1. As can be seen (dotted line in Fig. 1) the CI-I calculations including only the $3p\rightarrow ns$ and md excitations reproduce the experimental absorption spectrum very well, only the narrow structures, e.g., A', A'', B' and B'', seen in the experiment are absent.

The inset of Fig. 1 shows the narrow features A' and A'' of the absorption spectrum in detail. The CI-II calculations predict that there are few highly populated $3d^{-2}7p4d$ and $3d^{-2}5p6s$ CI states in this region. The data analysis revealed that the features exhibit a Fano line shape, which suggests that those states should be populated also by other channels. In general, the direct channel to double excited states is low, but it should be noted that also the CI between the $3p^{-1}ns/md$ and $3d^{-2}np(ns/md)$ states populates those states weakly and therefore interference effects resulting in the Fano line shape are possible. As can be seen from Table I, the CI-II approach does not reproduce the binding energies of the states A' and A'' as well as those of the singly excited states; however, the calculated intensities support the assignment. In addition, also the extracted linewidths of the structures A' and A'' (0.17 ± 0.05 eV) are in excellent agreement with the value of 0.18 eV, estimated from the natural linewidth of a single 3d hole state (88 meV) [19] and support the present assignment. However, more elaborate methods are needed to theoretically understand the nature of the structures in detail. According to CI-II calculations the faint structures B' and B'' at higher photon energies can be assigned as $3d^{-2}5p7s$ and $3d^{-2}5p6d$ states. The $3p_{3/2}^{-1}ns/md$ excited states interact quite strongly with the $3d^{-2}np(ns/md)$ states and lead to structures seen in the experimental spectrum. However, the $3p_{1/2}^{-1}ns/md$ states can be described almost purely within the one-electron picture and therefore similar structures are not expected above the $3p_{1/2}\rightarrow 5s$ excitation.

The present calculations produce the energy differences between the different 3p excitation energies well. The theoretical values for the lifetime widths of the Kr $3p^{-1}$ states differ slightly from the experimental results, but both show that the lifetime widths of the $3p_{3/2}^{-1}ns$ excited states are smaller than those of the $3p_{1/2}^{-1}ns$ excited states. The experimental lifetime widths are very close to the corresponding values of the $3p_{1/2,3/2}^{-1}$ states, 1.5 and 1.9 eV [9], respectively. Both the energies and the lifetimes obtained are possibly affected by the underlying unresolved $3p\rightarrow md$ excitations and by the opening of the $3p\rightarrow \epsilon s/\epsilon d$ continuum channels, which are reproduced in the fit using Gaussian lines.

B. Kr 3d photoelectron satellites

The experimental Kr 3d photoelectron shake-up satellite spectrum has been interpreted previously [20] on the basis of calculations of the energies of the states. The present calculations, based on Cowan's code, provide also detailed information about the intensity distribution of the shake-up spectrum. The Kr 3d photoelectron satellite spectrum of Fig. 2 was measured in the binding-energy region of the $3d^{-1}4s^{-1}ns$, $3d^{-1}4p^{-1}np(n\geqslant 5)$ states. According to energy calculations there are also some $3d^{-1}4p^{-1}ms(m=5,6)$ and $3d^{-1}4p^{-1}ld(l=4,5)$ conjugated satellite states. As the measurement was done well below the excitation energy of the first 3p resonance state, the intensity distribution is not affected by the resonant Auger channels. Due to the high resolution of the electron energy analyzer and the very narrow photon bandwidth, the structures of the shake-up spectrum could be observed in detail.

The theoretical photoelectron spectrum in the binding-energy region of interest was constructed using the $3d^{-1}4s^{-1}ns(n=5,6)$ and $3d^{-1}4p^{-1}mp(m=5$–$8)$ configurations. Relative intensities between the different $3d^{-1}4p^{-1}mp$ configurations were estimated using the overlap integrals $\langle 4p_i|mp_f\rangle$ of the wave functions, where i and f stand for the initial and final states, respectively. Calculations show that the strongly populated states in the binding-energy region of 112–122 eV [see Fig. 2] belong to the $3d^{-1}4p^{-1}mp(m=5$–$8)$ configurations. Figure 2 shows that the theoretical model reproduces the main structures and also the energy distribution of the spectrum very well (a shift of 0.84 eV is used in Fig. 2), but underestimates the shake probabilities to the $3d^{-1}4p^{-1}mp(m\geqslant 6)$ states. Two clear structures around 126 eV were assigned to the $3d^{-1}4s^{-1}5s$ states. The correlation between the $4s$ hole with $4p^{-2}kd(k=4,5,6)$ states was included in the calculation of the $3d^{-1}4s^{-1}ns(n=5,6)$ states. The correlation decreases both the binding energy and the intensity of the $3d^{-1}4s^{-1}ns$ states and distributes intensity to $3d^{-1}4p^{-2}kdns$ states. The numerous $3d^{-1}4p^{-1}kdns$ states (730 states for each n if k is limited to values 4, 5, and 6) are not presented in the theoretical spectrum (columns in Fig. 2) as the intensity is distributed into a long energy range quite evenly but the effect of correlation to the $3d^{-1}4s^{-1}ns$ states is still taken into account. In the case of the $3d^{-1}4p^{-1}ld(l=4,5)$ and $3d^{-1}4p^{-1}ms(m=5,6)$ conjugated satellite states the intensity calculations were omitted as these states are supposed to

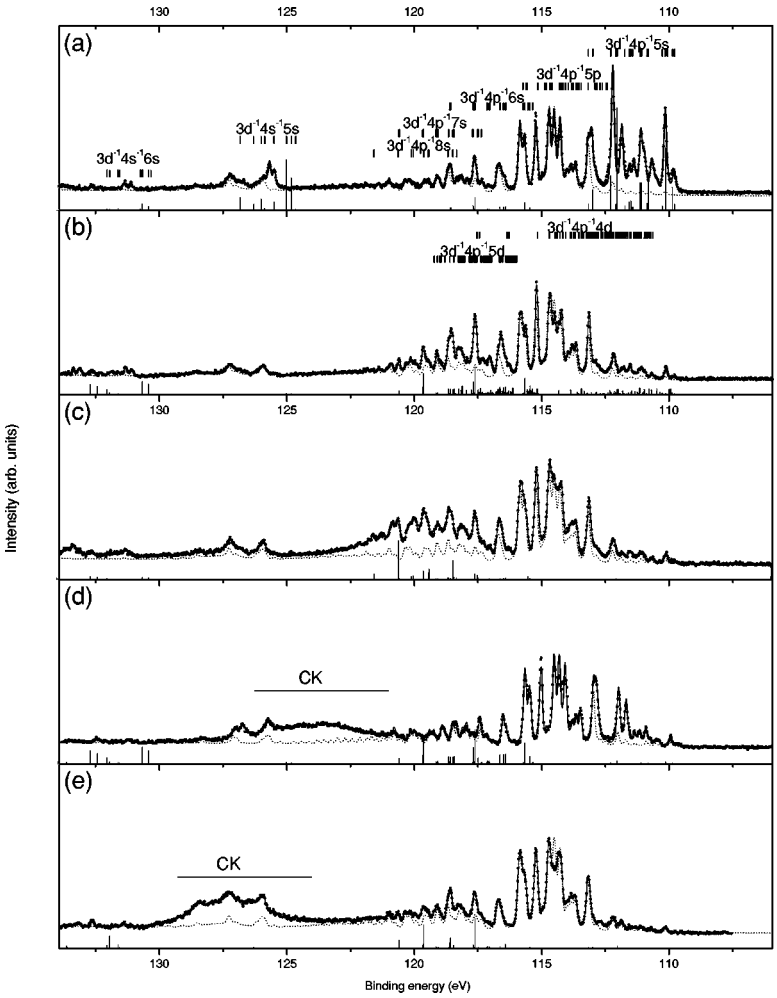

FIG. 3. The electron spectra of Kr measured at photon energies corresponding to the (a) $3p_{3/2}\rightarrow 5s$, (b) $3p_{3/2}\rightarrow 6s/3p_{3/2}\rightarrow 4d$, (c) $3p_{3/2}\rightarrow 7s/3p_{3/2}\rightarrow 5d$, (d) $3p_{1/2}\rightarrow 5s$, and (e) $3p_{1/2}\rightarrow 6s/3p_{1/2}\rightarrow 4d$ excitations. In all figures, dots present experimental data, the thick lines a fit (either a least squares or a spline) (see text for details), and the dotted line the photoelectron spectrum measured below Kr $3p$ excitations, whereas columns show the theoretical resonant Auger spectrum. The main structures of the spectrum are assigned according to the HF calculations.

be populated weakly. Figure 2 clearly shows that the structures of the experimental spectra are reproduced very well with the present calculations.

C. Resonant Auger decay

In order to verify the assignment of the main structures of the absorption spectrum and to obtain information about different decay paths originating from $3p\rightarrow nl$ excitations, resonant Auger spectra were recorded in the binding-energy region of the $3d^{-1}(4p/4s)^{-1}nl$ states. In the case of the $3p_{3/2}$ excitations, the photon energy was set to correspond to the peaks *A*, *B* and *C*. The Kr $3p_{1/2}\rightarrow nl$ excitations are weaker than the corresponding $3p_{3/2}\rightarrow nl$ excitations by approximately the statistical factor of 0.5. Therefore the resonant Auger decay was studied only at photon energies corresponding to the two strongest peaks, *a* and *b*. Resonant Auger spectra corresponding to different photon energies, and therefore different excitations, are presented in Fig. 3 in comparison with the $3d$ shake-up photoelectron spectrum.

The direct photoionization channel populates mostly the $3d^{-1}4p^{-1}np(n\geqslant 5)$ and $3d^{-1}4s^{-1}ns$ states whereas the resonant Auger channel following the $3p\rightarrow ns$ excitations are expected to populate mostly the $3d^{-1}4p^{-1}ns$ and $3d^{-1}4s^{-1}ns$ states. Therefore clear changes should occur in the binding-energy region of interest when the photon energy is set on or off the different resonances. In addition, resonant Auger decay provides a way to study especially $3d^{-1}4p^{-1}ns$ conjugated satellite shake-up states as they were found to be very weakly or not at all populated in direct photoionization.

Theoretical resonant Auger spectra and shake probabilities were calculated using Cowan's code by neglecting CI in both the initial and the final states. The theoretical shake-up probabilities of the resonant Auger decay spectra were also calculated as overlaps between the ns wave functions in the core-excited and final states of Auger decay. According to the present calculations, the main decay path following $3p\rightarrow ns$ excitations leads to $3d^{-1}4p^{-1}ns$ states.

The experimental spectrum corresponding to $3p_{3/2}\rightarrow 5s$ excitation (peak *A* in Fig. 1) is reproduced by the calculations very well. The spectator decay to $3d^{-1}4p^{-1}5s$ states dominates, as suggested by theory but shake-up transitions to $3d^{-1}4p^{-1}6s$ states have a significant probability, about 11%, which agrees exactly with the theoretical value. The experiment also agrees with the prediction that the population of the $3d^{-1}4p^{-1}ns$ states increases much more than that of the $3d^{-1}4s^{-1}ns$ states [see Fig. 3(a)]. As there are no underlying $3p_{3/2}\rightarrow md$ excitations, the decay originating from the $3p_{3/2}^{-1}5s$ state allows us to identify the $3d^{-1}4p^{-1}5s$ and $3d^{-1}4p^{-1}6s$ states and to conclude that

the calculations are capable of reproducing the experiment.

When the photon energy was set to correspond to peak *B* in the absorption spectrum, the $3d^{-1}4p^{-1}6s$ states and corresponding $3d^{-1}4p^{-1}7s$ shake-up states were populated. However, the decay populated also some other states in the same region. The calculations show that there are $3d^{-1}4p^{-1}4d$ states in the region. The population of such states also confirms the existence of the $3p^{-1}md$ states in the absorption spectrum. Setting the photon energy to higher $3p_{3/2}$ excitations allows us to identify higher $3d^{-1}4p^{-1}ns(n\geqslant 5)$ and $3d^{-1}4p^{-1}md(m\geqslant 4)$ states even though strong shake-up and shake-down transitions distribute intensity into a quite long energy range.

The broad structure [labeled as CK in Figs. 3(d) and 3(e)] in the electron spectrum corresponding to the $3p_{1/2}^{-1}nl$ excitation is caused by the $3p_{3/2}^{-1}\rightarrow 3d^{-1}4p^{-1}$ Coster-Kronig decay. The line narrowing effect caused by the Auger resonant Raman effect is well demonstrated, for instance, in Fig. 3(d) as, e.g., the $3d^{-1}4p^{-1}5s$ states are populated by resonant Auger CK and $3d^{-1}4p^{-1}$ states by normal CK decay. The effect of the resonant Auger decay is clear, in particular the $3d^{-1}4p^{-1}ns$ states are populated but not as strongly as in the case of decay following the $3p_{3/2}$ excitations. The overlapping CK transitions hamper the analysis of the $3d^{-1}4s^{-1}5s$ states but the change in the population of those states is nevertheless visible.

The absorption structures labeled as A' and A'' were also studied by measuring electron spectra at the corresponding photon energies. Careful analysis of the corresponding resonant Auger spectrum at the binding-energy region of the $3d^{-1}4p^{-1}np$ and $3d^{-1}4s^{-1}ns$ states did not show any changes in the relative intensities of the states. The lack of effects in the decay spectrum can, however, be understood as the $3d^{-2}5s6p$ and $3d^{-2}7p4d$ states are very weakly populated compared to the neighboring $3p_{3/2}^{-1}ns$ states, and they may also decay predominantly to other states than those under study.

IV. CONCLUSIONS

The excitation energies and the linewidths of the Kr $3p^{-1}ns(n=5-7)$ states were determined from the high-resolution absolute absorption spectrum measured at the $3p$ ionization threshold. Novel structures A', A'', B' and B'' were detected in the absorption spectrum. They were explained by the configuration interaction between the $3p^{-1}ns(n=5-7)$, $3p^{-1}md(m=4-6)$ and $3d^{-2}np(ns/md)$ states. More elaborate calculations are, however, needed to reproduce the behavior of those CI states. The resonant Auger decay of the excited states was also studied in detail. The present experiment confirms the theoretical assignment of the features of the absorption spectrum. From the resonant Auger-electron spectra it is evident that structures *A* and *a* in the absorption spectrum are due to the $3p\rightarrow ns$ transitions as suggested earlier by Ohno [8]. Resonant Auger decay also reveals that in the absorption spectrum there are underlying $3p\rightarrow md$ excitations in the region of the peaks *B*, *C*, *b*, and *c*. The Kr $3d$ photoionization shake-up satellite structures were also resolved in the region of the $3d^{-1}4p^{-1}np$, $3d^{-1}4s^{-1}ns$ shake-up states. The theoretical calculations reproduced the structures of the experimental spectrum very well.

ACKNOWLEDGMENTS

The staff of ELETTRA are acknowledged for assistance during the measurements. This work was supported by the European Union (Project No. ERB FMGE CT95 0022-A.No.1), the Research Council for the Natural Sciences of the Finnish Academy, and the Tauno Tönninki Foundation.

[1] S. Svensson, N. Mårtenson, E. Basilier, P.Å. Malmquist, U. Gelius, and K. Siegbahn, Phys. Scr. **14**, 141 (1976).
[2] M. Ohno and G. Wendin, Phys. Scr. **16**, 299 (1977).
[3] G. Wendin and M. Ohno, Phys. Scr. **14**, 148 (1976).
[4] A. Kivimäki, H. Aksela, J. Jauhiainen, M. Kivilompolo, E. Nõmmiste, and S. Aksela, J. Electron Spectrosc. Relat. Phenom. **93**, 89 (1998).
[5] S. Heinäsmäki, H. Aksela, A. Kivimäki, and S. Fritzsche (unpublished).
[6] T. Hayaishi, Y. Morioka, T. Akahori, M. Watanabe, A. Yagishita, and M. Nakamura, Z. Phys. D: At., Mol. Clusters **4**, 25 (1986).
[7] I.T. Steinberger, C.M. Teodorscu, D. Gravel, R. Flesch, B. Wasserman, G. Reichardt, C.W. Hutchings, A.P. Hitchcock, and E. Rühl, Phys. Rev. B **60**, 3995 (1999).
[8] M. Ohno, Phys. Rev. A **51**, 1042 (1995).
[9] T. Matsui, H. Yoshii, A. Higurashi, E. Murakami, T. Aoto, T. Onuma, Y. Morioka, A. Yagishita, and T. Hayaishi, J. Phys. B **35**, 3069 (2002).
[10] J. Jauhiainen, A. Kivimäki, S. Aksela, O-P. Sairanen, and H. Aksela, J. Phys. B **28**, 4091 (1995).
[11] S. Brünken, Ch. Gerth, B. Kanngießer, T. Luhmann, M. Richter, and P. Zimmerman, Phys. Rev. A **65**, 042708 (2002).
[12] J. Karvonen, A. Kivimäki, H. Aksela, S. Aksela, R. Camilloni, L. Avaldi, M. Coreno, M. de Simone, and K.C. Prince, Phys. Rev. A **59**, 315 (1999).
[13] R.R. Blyth, R. Delaunay, M. Zitnik, J. Krempasky, R. Krempaska, J. Slezak, K.C. Prince, R. Richter, M. Vondracek, R. Camilloni, L. Avaldi, M. Coreno, G. Stefani, C. Furlani, M. de Simone, S. Stranges, and M.-Y. Adam, J. Electron Spectrosc. Relat. Phenom. **101-103**, 959 (1999).
[14] J.A.R. Samson, Z.X. He, L. Yin, and G.N. Haddad, J. Phys. B **27**, 887 (1994).
[15] M. de Simone, M. Coreno, M. Alagia, R. Richter, and K. Prince, J. Phys. B **35**, 61 (2002).
[16] G.C. King, M. Tronc, F.H. Read, and R.C. Bradford, J. Phys. B **10**, 2479 (1977).
[17] J. Jauhiainen, A. Ausmees, A. Kivimäki, S.J. Osborne,

A.Naves de Brito, S. Aksela, S. Svensson, and H. Aksela, J. Electron Spectrosc. Relat. Phenom. **69**, 181 (1994).

[18] R.D. Cowan, *The Theory of Atomic Structure and Spectra* (University of California Press, Berkeley, 1981).

[19] M. Jurvansuu, A. Kivimäki, and S. Aksela, Phys. Rev. A **64**, 012502 (2001).

[20] S. Svensson, B. Eriksson, N. Mårtensson, G. Wendin, and U. Gelius, J. Electron Spectrosc. Relat. Phenom. **47**, 327 (1988).